J. Mt. Sci. (2014) 11(2): 371-383 e-mail: jms@imde.ac.cn http://jms.imde.ac.cn
DOI: 10.1007/s11629-013-2790-6

Effect of Lithology and Structure on Seismic Response of Steep Slope in a Shaking Table Test

LIU Han-xiang[1], XU Qiang[1]*, LI Yan-rong[2]

1 State Key Laboratory of Geohazard Prevention and Geoenvironment Protection, Chengdu University of Technology, Chengdu 610059, China

2 AGECON Ltd., Hong Kong, China

**Corresponding author, e-mail: xuqiang_68@126.com; First author, e-mail: hxliu_86@163.com*

Citation: Liu HX, Xu Q, Li YR (2014) Effect of lithology and structure on seismic response of steep slope in a shaking table test. Journal of Mountain Science 11(2). DOI: 10.1007/s11629-013-2790-6

Abstract: Studies on landslides by the 2008 Wenchuan earthquake showed that topography was of great importance in amplifying the seismic shaking, and among other factors, lithology and slope structure controlled the spatial occurrence of slope failures. The present study carried out experiments on four rock slopes with steep angle of 60° by means of a shaking table. The recorded Wenchuan earthquake waves were scaled to excite the model slopes. Measurements from accelerometers installed on free surface of the model slope were analyzed, with much effort on time-domain acceleration responses to horizontal components of seismic shaking. It was found that the amplification factor of peak horizontal acceleration, R_{PHA}, was increasing with elevation of each model slope, though the upper and lower halves of the slope exhibited different increasing patterns. As excitation intensity was increased, the drastic deterioration of the inner structure of each slope caused the sudden increase of R_{PHA} in the upper slope part. In addition, the model simulating the soft rock slope produced the larger R_{PHA} than the model simulating the hard rock slope by a maximum factor of 2.6. The layered model slope also produced the larger R_{PHA} than the homogeneous model slope by a maximum factor of 2.7. The upper half of a slope was influenced more seriously by the effect of lithology, while the lower half was influenced more seriously by the effect of slope structure.

Keywords: Seismic response; Shaking table test; Topography; Lithology; Slope structure

Received: 27 May 2013
Accepted: 30 October 2013

Introduction

Tens of thousands of secondary geo-hazards such like landslides, debris flows, rock falls, rock avalanches were triggered by the 2008 Wenchuan earthquake in the Longmen Mountains of China (Huang and Li 2008), and caused about 20,000 deaths and great property loss, accounting for one third of the total loss in the earthquake (Chen et al. 2009). At least 257 landslide dams were also generated by the quake according to the preliminary interpretation of Cui et al. (2009), with the largest one, Tangjiashan landslide having a storage capacity of 302 million m^3. These geohazards have produced a long-term risk in the form of disaster chains, such as with debris flows and floods due to dam break (Huang and Fan 2013). The earthquake area is characterized by rugged topography, steep high mountains, deep valleys and complicated geological structures. It is extremely meaningful to explore how the geological and topographic conditions influence or control the occurrence of geological disasters, from the view of engineering for disaster reduction.

The post-earthquake researches indicate a controlling role of lithology and rock structure of a slope, among diverse factors, in contributing to the

development and distribution modes of the hazards and the formation mechanisms. Xu (2009) categorized landslides occurring in the earthquake area into three types, i.e., loose deposit landslide, soft rock landslide and hard rock landslide. Chigira et al. (2010) further concluded that hard rock slopes produced more landslides relative to the soft rock slopes. Slopes composed of jointed or layered structures even caused ejection towards the free face or movement over long distance, like the Donghekou Landslide, the Woqian Landslide and the Shibangou Landslide (Xu et al. 2009). Before the 2008 Wenchuan earthquake, the 1994 Northridge earthquake, California, also caused rock falls and rock slides with 90 percent of 11,000 landslides over an area of about 10,000 km^2 (Harp and Jibson 1996). Keefer (1984) concluded that disrupted rock avalanches and rock falls were the most abundant hazards responsible for the great loss in a strong earthquake.

Besides the effect of lithology and slope structure, topographic effect is another factor responsible for the slope failure in an earthquake. During the 2008 Wenchuan earthquake, landslides accumulated at the slope crests, the transition section of slope gradients and thin mountain ridges (Huang and Li 2008), and the landslide concentration (landslides/km^2) showed an increase with slope angle and reached its peak in the category of 50°-60° (Qi et al. 2010). Based on the historical earthquakes, a systematic review on topography effects was made by Geli et al. (1988), who compared the theoretical and experimental results, and found qualitative agreement about the amplification at mountain tops. However, the time domain crest/base amplification ratios remained below 2 in theoretical results, while the corresponding values reached around 8 in experimental results. Moreover, the theoretical crest/base spectral amplification ranged between 2 and 7 for other complex models, while the experimental spectral amplification could reach 30. Effects of lithology, slope structure and topography always interact with each other to produce the complex slope response to seismic waves. Harp and Jibson (2002) found it was the anomalously strong shaking in Pacoima Canyon resulting from topographic amplification that explained the spatial distribution of rock falls. Bozzano et al. (2011) pointed out joint conditions of the involved rock mass were responsible for the seismic amplification of the landslide-prone volume based on a finite difference numerical modeling of the Scilla landslide.

Field observation, numerical calculation and physical model test are the main methods in researching the seismic response of rock slope. Del Gaudio and Wasowski (2007) observed the directional differences in shaking energy by a factor of 2-3 based on their long-term field monitoring in a potential landslide. However, they also conveyed that the random occurrence of an earthquake made it difficult to collect enough earthquake recordings needed for a satisfactory evaluation of seismic response. For numerical modeling, how to simulate strength properties of discontinuities and intact rock bounded by discontinuities and slope geometry is still a challenge encountered by researchers (Hatzor et al. 2004; Ducellier and Aochi 2012). Shaking table model tests have been widely adopted in studies on soil slope responses to seismic waves (Yang et al. 2002; Ling et al. 2005; Lin and Wang 2006; Wang and Lin 2011). Shimizu et al. (1988) conducted three kinds of two-dimensional model tests to investigate the dynamic failure modes of rock slopes. The maximum amplification of about 300% was observed in accelerometers embedded at the top of a shaking table model of 600 mm long and 400 mm high. Nowadays, studies in this particular field are carried out by using advanced shaking tables, which allow large models and diverse waves to be investigated (Liang et al. 2005; Dong et al. 2011; Ye et al. 2013).

In the present study, a shaking table with six degrees of freedom (three translational motions and three rotational motions) was used to excite four model slopes with steep angle of 60°, differing from lithology and rock structure. Each model slope was instrumented by five accelerometers at different elevations on the free surface. The model slopes were mainly subjected to a broad range of shaking levels, in horizontal, vertical, and their resultant directions, scaled from the 2008 Wenchuan earthquake waves. Characteristics of horizontal component response of slope to seismic waves were discussed in detail in terms of the topographic effect, based on recordings from the installed accelerometers in each model slope. After that, influence of lithology and slope structure on

the topographic effect were explored separately, by comparing responses between two models composed of different lithologies and between two models composed of different slope structures.

1 Test Program

1.1 Model materials

Two model slopes with homogeneous materials were prepared in a model container (Figure 1a), whilst another two model slopes with horizontally layered materials were prepared in the other container (Figure 1b). The left model slopes in Figure 1a and Figure 1b were composed of materials of low strength. They were used to simulate rock slopes with homogeneous and layered soft rocks, and were conveniently represented by the HS model and LS model respectively. The right two model slopes were composed of materials of high strength and were used to simulate rock slopes with homogeneous and layered hard rocks, and were conveniently represented by HH model and LH model respectively. The Niumiangou Landslide in the Wenchuan county and the Zhengjiashan Landslide in the Pingwu county, both triggered by the 2008 Wenchuan earthquake, were used as the prototypes in terms of their lithology and structure. They occurred in hard rock stratum (granite) and soft rock stratum (slate), respectively (Xu et al. 2009). For simplification purpose, two model slopes were structured only by horizontal layers in the present study. In order to explore the structure effect on seismic slope responses, the other two model slopes composed of homogeneous materials were tested simultaneously. Only the lateral view of two homogeneous models in a container is given by Figure 2, since the lateral view of two layered models is almost the same to Figure 2 except the horizontal interfaces.

The Buckingham's π theorem is based on dimensional analysis and gives the transformation from a function of dimensional parameters ($f(q_1, q_2, q_3 \ldots q_n) = 0$) to a related function of dimensionless parameters ($F(\pi_1, \pi_2, \pi_3 \ldots \pi_4) = 0$) (Louis 1957; Curtis 1982). In the present study, soil density ρ, elasticity modulus E

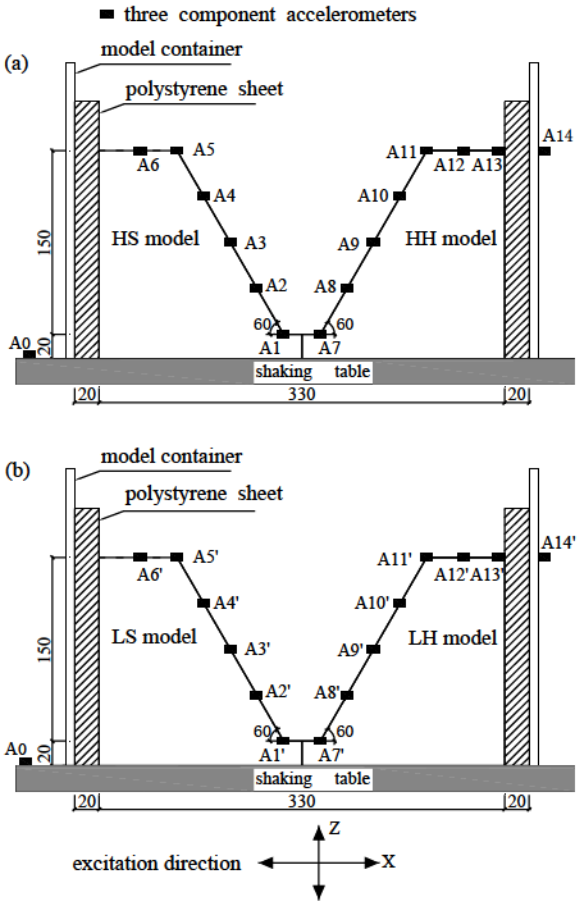

Figure 1 Set-up of the shaking table model slopes: (a) homogeneous soft rock (HS) model and hard rock (HH) model; (b) layered soft rock (LS) model and hard rock (LH) model (Unit: cm).

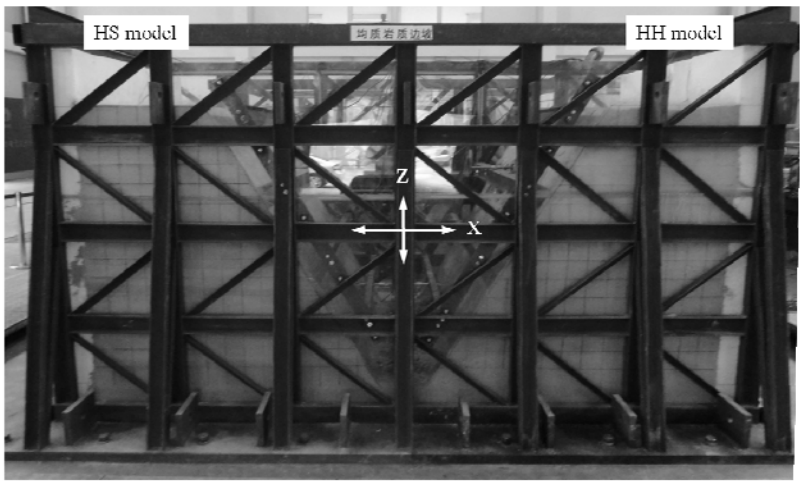

Figure 2 Lateral view of two homogeneous model slopes in a container: the left model simulated soft rock slope (HS model); the right model simulated hard rock slope (HH model).

and time t were selected as the controlling parameters, and their scale factors were 1.0, 32.6 and 4. The scale factor of length C_L=22.9 indicated the height of the prototype slope was 34.3 m. Based on the controlling quantities, the π terms for the F function and the corresponding scale factors of the other key parameters were calculated in Table 1.

Table 1 The π terms and scale factors of key parameters. C_parameters =Controlling parameters.

Dimensionless π terms	Scale factor	Dimensionless π terms	Scale factor
C_ parameter	$C_\rho = 1$	$\pi_\sigma = \sigma/(E\,\varepsilon)$	$C_\sigma = C_E\,C_\varepsilon = 22.8$
C_ parameter	$C_E = 32.6$	1	$C_\varepsilon = 0.7$
C_ parameter	$C_t = 4$	$\pi_f = f/t$	$C_f = C_t^{-1} = 0.25$
$\pi_L = L/(E^{0.5}\rho^{-0.5}t)$	$C_L = C_E{}^{0.5}C_\rho{}^{-0.5}C_t = 22.9$	$\pi_u = u/(L\,\varepsilon)$	$C_u = C_L\,C_\varepsilon = 16$
1	$C_\mu = 1$	$\pi_v = v/(u\,t^{-1})$	$C_v = C_u\,C_t^{-1} = 4$
$\pi_c = c/(E\,\varepsilon)$	$C_c = C_E\,C_\varepsilon = 22.8$	$\pi_a = a/(u\,t^{-2})$	$C_a = C_u\,C_t^{-2} = 1$
1	$C_\Phi = 1$		

Table 2 Physical and mechanical parameters of the prototype slopes (P) and the model slopes (M)

Lithology		Density ρ (10^3kg/m^3)	Cohesion c (kPa)	Frictional angle Φ (°)	Elastic modulus E (MPa)	Poisson's ratio μ
Hard rock	P	2.7	1600	39	8940	0.23
	M	2.52	83.4	36.5	253.2	0.26
Soft rock	P	2.48	520	33.8	1900	0.31
	M	2.4	37.1	34.9	50.2	0.3
Interface			18	19.2		

Barite powder, quartz sands, gypsum, glycerol and water were mixed in weight proportions of 32:54:7.5:1.5:5.5 to produce the high strength material of model slopes which simulated prototype hard rock (with the saturated uniaxial compression strength of 105.5 Mpa), while a mixture of the same components in proportions of 32:56:6:1:7 were to make the low strength materials, which simulated the prototype soft rock (with the saturated uniaxial compression strength of 10.6 Mpa). Note that the above proportions were determined through try and error. The barite powder (maximum particle size of 0.074 mm) and quartz sands (0.074 to 0.85 mm) work as fines and coarse aggregates in the mixture, and the gypsum and water work together as cement. Glycerol was used to slow down the curling of the mixture, in order to achieve the desired strength. Direct shear tests in accordance with Chinese Standard for Soil Test Method (GB/T 50123-1999) were conducted to obtain the cohesions and internal friction angles of the mixture, and uniaxial compression strength tests in accordance with Standard for Soil Test Method (GB/T 50123-1999) were conducted to obtain the elasticity modulus. The mechanical properties of the interfaces between layers were obtained through direct shear tests (GB/T 50123-1999). The properties of materials for model slopes are listed in Table 2.

1.2 Model preparation

Every two model slopes were prepared in a steel model container with a length of 3.7 m, width of 1.5 m, and height of 2.1 m. Rigid container have been used in many studies of slope, such as Hong et al. (2005), Ling et al. (2005), Wartman et al. (2005), and Lin and Wang (2006). To minimize the influences of boundary of the model container on the input seismic waves, an absorber made of polystyrene sheet wrapped with polyethylene film was placed on two sides of each container, perpendicular to the excitation (X-) direction in Figure 1. According to Withman and Lambe (1986), soil close to rigid boundary responded differently than soil near the middle of the model, but nevertheless concluded that "reasonably correct" physical model test data could be obtained in rigid containers.

The height of each model slope was 1.5 m. A 20 cm thick foundation, with the same material to the model slope was laid at the bottom of the model container. The model slope was prepared by wet pouring and compacting, layer by layer, a certain volume of mixed material into a 15 cm thick layer. Such a method ensured the desired unit weights as listed in Table 2. For the layered model slopes, 3 mm thick fine sands pigmented in red were spread on the contact surface (interface) between layers. The interface is designed only to make the layer structure of a slope, and the effect of its properties (thickness, dip angle, strength) on seismic slope response is not much concerned in the present study. During build-up of the model slopes, a

modeler was used to keep the slope angle at the designated 60°. The final products were two model slopes standing face to face in each model container, forming a U-shaped valley as shown in Figure 1 and Figure 2.

1.3 Test set-up

The shaking table used in this study has a capacity of 60 t, and the maximum working frequency is 80 Hz. The size of the table is 6.0 m by 6.0 m, and allows the placement of two model containers in this test. The ranges of displacement are -150 to +150 mm in two orthogonally horizontal directions and -100 to +100 mm in the vertical direction. The ranges of acceleration under full load are -1 to +1 g in two orthogonally horizontal directions and -0.8 to + 0.8 g in the vertical direction.

As shown in Figure 1, five three-component accelerometers with a measuring capacity of up to 6.0 g were installed at different elevations on the surface of each model slope. In order to minimize the longitudinal (X-) boundary effects, sensors were placed along the middle line from toe to top of the model. An accelerometer (A0 in Figure 1) was fixed on the bottom plate of the shaking table to check the excitation waves.

1.4 Input motions

The horizontal (EW) and vertical (UD) components of the accelerations recorded at the Wolong seismic station during the 2008 Wenchuan earthquake were scaled for the model loading inputs, and the seismograms were obtained from the release by the China Earthquake Networks Center. The Wolong station is located in Wolong town of Wenchuan County. The altitude on the station ground is 919 m above see level and altitude on the top of the mountain nearby is 3,187m. The overlying soils at the station are mainly composed of Quaternary alluvial and diluvial gravels and pebbles. In the Wenchuan earthquake, the station had the shortest epicentral distance of about 23 km and recorded the maximum peak ground accelerations, of which the EW- and UD-components were 957.7 gal and 948.1 gal, respectively (Wen et al. 2010). The ground motion duration of both components was 108 s, and the corresponding dominant frequencies were 2.4 Hz and 8.1 Hz. In the test, the EW- and UD-recordings were proportionally scaled into the required horizontal and vertical loading inputs in time domain: all input waves had the duration of 27 s according to the time scale factor of 4 in Table 1, and the input amplitudes for each kind of loading direction were from 0.1 to 1.0 g at an interval of 0.1 g. As shown in Figure 1, the model slopes were excited from the bottom, respectively, by the above horizontal (X-direction), vertical (Z-direction) waves and their combinations.

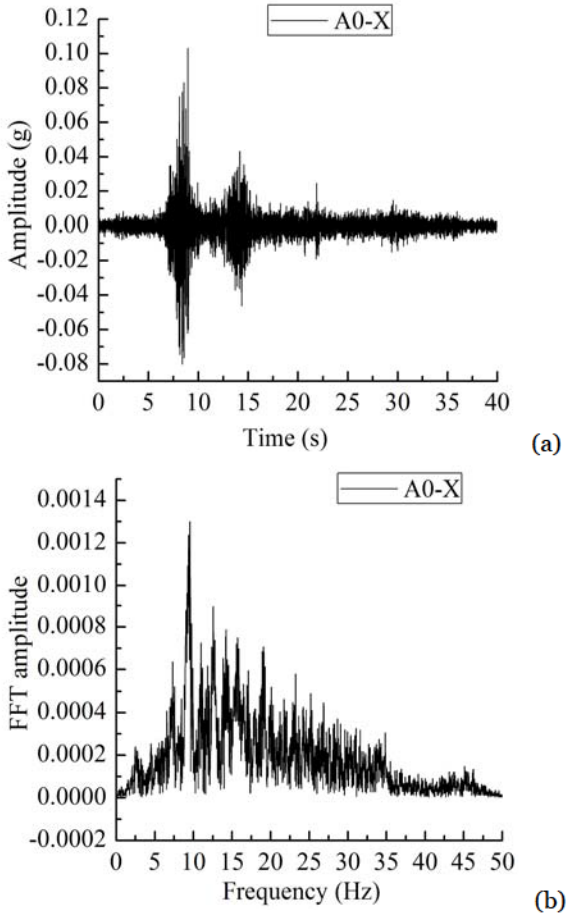

Figure 3 The excitation acceleration for the X-direction shaking: (a) time history, and (b) Fourier amplitude spectrum.

The input wave of horizontal component collected on the table A0 is shown in Figure 3, together with its Fourier amplitude spectrum, since only horizontal component response will be analyzed in the present paper. Figure 3 shows the dominant frequency of horizontal input waves is 9.6 Hz and coincides with the similitude relations (4 times of the dominant frequency of the EW-

component). Besides, sine waves with excitation frequency from 5 Hz to 15 Hz were also input at the base of the model slopes in X- and Z- direction shakings. The loading sequence of the test is given in Figure 4.

The test started with exciting the model slopes by a White Noise wave with a flat Fourier spectrum in all frequencies (< 50 Hz) so as to obtain the initial dynamic characteristics of the model slope. Based on the responding signals in the model under White Noise excitation, transfer function of the model was obtained using Matlab's function *tfestimate*() in Signal Processing Toolbox. Figure 5 gives the transfer functions of the X- component excitation, calculated for different monitoring points, A1', A2', A3', A4' and A5' in the LS model. The average dominant frequency identified from Figure 5 was regarded as the fundamental resonance frequency of the LS model slope at the first stage of the test. The resonance frequency of the LS model for X-direction shaking was 19.5 Hz. In the same way, the initial resonance frequencies of the HH model, HS model and LH model were 32.5 Hz, 22 Hz and 28.5 Hz. Thus, no resonance would occur as the dominant frequency of input wave (9.6 Hz in horizontal) during the present tests are totally different from the natural frequencies of the model slopes. Another six White Noise excitations were used to excite the model slopes at different stages of the test, as shown in Figure 4. Seven White Noise excitations are represented by White 1, 2, ... and 7.

2 Results and Discussions

In Figure 1, a column of three-component accelerometers were arranged along the middle line from the toe to the top of each slope surface. Baseline correction and Butterworth low-pass filtering were conducted on the raw dataset to correct it in the Matlab 8.0, before any further analysis. Only horizontal (X) component response under the horizontal (X) direction shaking of the Wenchuan wave was analyzed in the present paper. Three dimensionless ratios were used to study the X-component responses of the model slopes in time domain.

Amplification factor

The amplification factor (R) was defined by the ratio of the peak horizontal acceleration (PHA) measured in any monitoring point to that measured on the bottom plate of the table. Such a definition makes R > 1.0 indicate real amplification, R = 1.0 non-amplification, and R <1.0 attenuation.

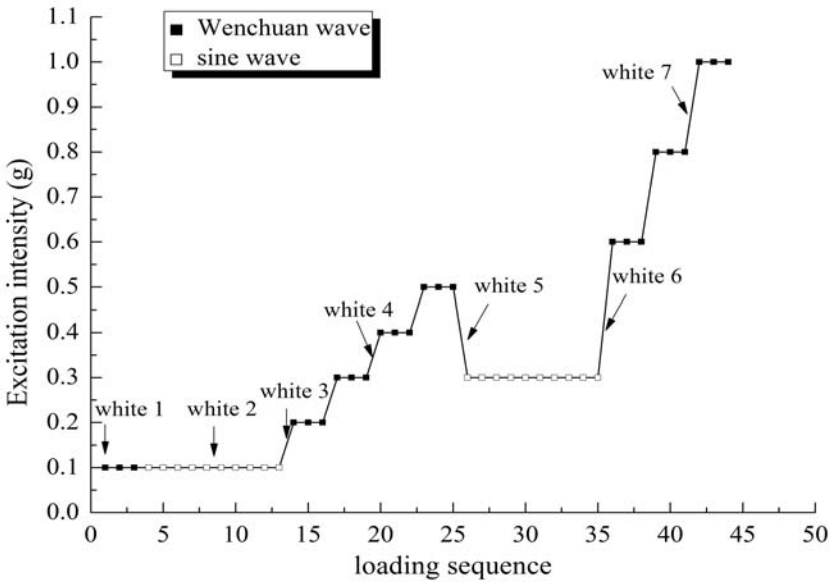

Figure 4 Loading sequence of the shaking table test (the arrows indicate the time when the White Noise wave excites the models).

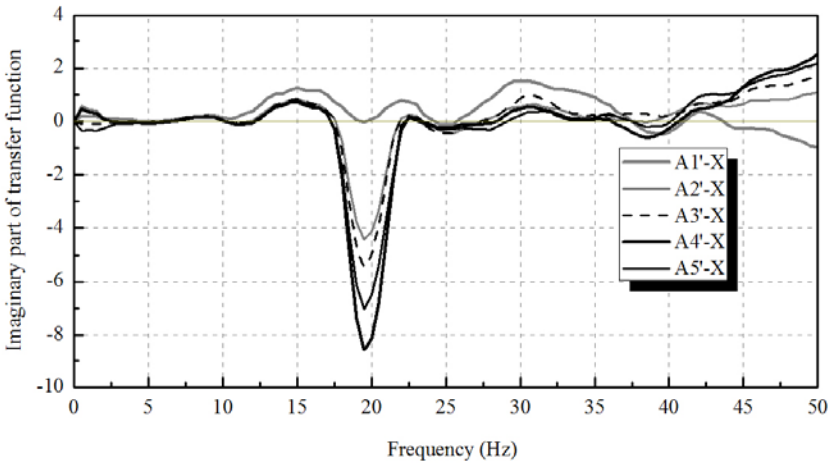

Figure 5 Transfer function under X- direction shaking based on the White Noise excitation at the first stage of test for the LS model.

PHA was obtained by taking the maximum absolute value of the measured horizontal component acceleration in time domain for each monitoring point. The relative elevation (h/H) was defined as the ratio of height (h, measured from the toe of the model slope) of any monitoring point to the total height (H) of the slope.

Lithology factor

The lithology factor (R_{lith}) was defined by the ratio of PHA of the soft rock model slope to that of the hard rock model slope for two monitoring points in the same elevation. Separately, the factor R_{lith}^1 was used for the ratio between two homogeneous model slopes (e.g. A5 and A11 in Figure 1), and R_{lith}^2 was used for the ratio between two layered model slopes (e.g. A5' and A11' in Figure 1).

Structure factor

The structure factor (R_{stru}) was defined by the ratio of PHA of the layered model slope to that of the homogeneous model slope for two monitoring points in the same elevation. Separately, the factor R_{stru}^1 was used for the ratio between two soft rock model slopes (e.g. A5 and A5' in Figure 1), and R_{stru}^2 was used for the ratio between two hard rock model slopes (e.g. A11 and A11' in Figure 1).

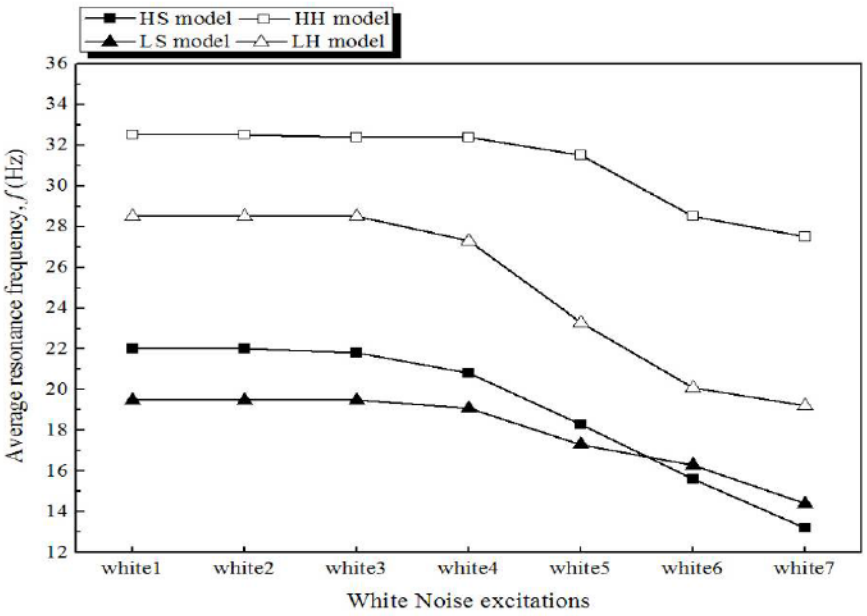

Figure 6 Average resonance frequency, f, of each model slope under X-direction shaking based on the White Noise excitation at different stages of test.

2.1 Dynamic characteristics

The fundamental resonance frequencies of four model slopes under seven White Noise excitations, from White 1 to White 7, are shown in Figure 6. It can be seen the resonance frequency decreased from 22 to 13.2 Hz for the HS model, 32.5 to 27.5 Hz for the HH model, 19.5 to 14.4 Hz for the LS model, and 28.5 to 19.2 Hz for the LH model. According to Beresnev et al. (1995), assuming the model slope as a geological layer, the fundamental resonance frequency f of the model, the shear velocity V of the slope material and the layer thickness H follow the relationship $V = f \times 4H$. The decrease of resonance frequency f indicates the decrease of the shear velocity V, and further reflects the internal structure of the model is becoming more loose. In Figure 6, The sharp drop of the resonance frequency began in White 5 excitation for the HS, LS and LH modes, in White 6 excitation for the HH model, which indicated a sudden deterioration of the internal structure of each model slope when the excitation intensity of the Wenchuan wave increased up to 0.5 g, according to the loading sequence of Figure 4. Another observation is that the magnitude of the resonance frequency was slightly different between two model slopes composed of the same materials but different structures (i.e. the HS and LS models, the HH and LH models), and was obviously different between two model slopes with the same structure but different materials (i.e. the HS and HH models, the LS and LH models). The hard rock model slope had the larger shear velocity V than the soft rock model slope, consequently, it obtained the higher resonance frequency f. Compared with the homogeneous materials, the horizontal layers composing the model slope reduced the shear stiffness of the model, and so caused a lower resonance frequency.

2.2 Topographic effect

Figure 7 gives the amplification factors of peak horizontal accelerations (R_{PHA}) at different

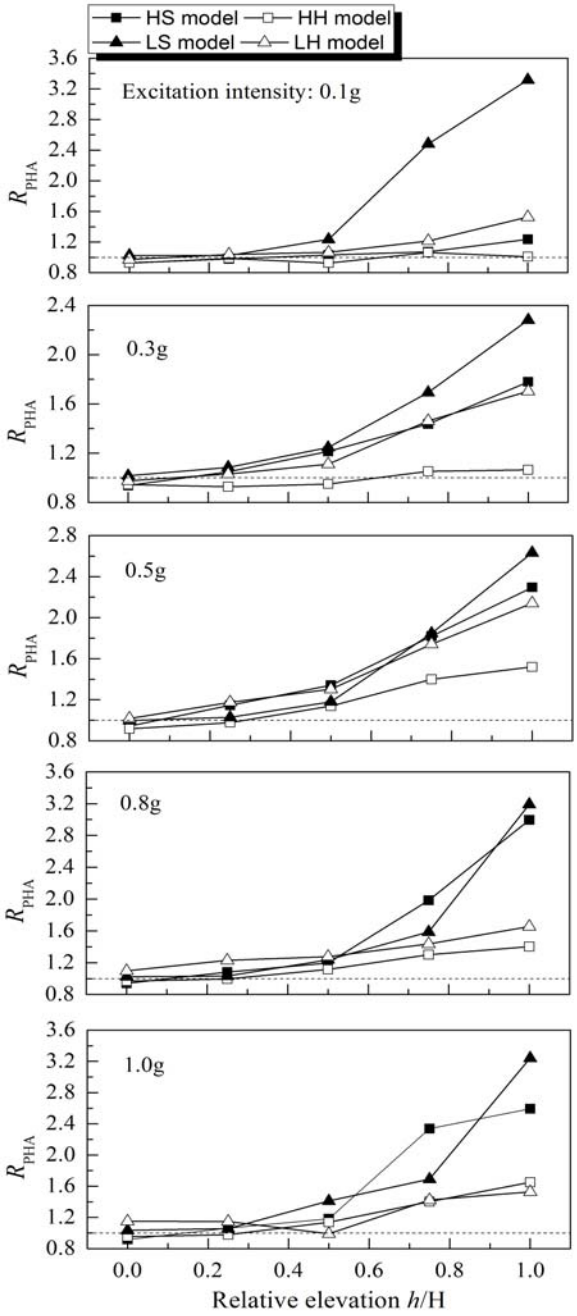

Figure 7 *PHA* amplification factor, R_{PHA}, under X-direction shaking versus relative elevation h/H.

elevations, A1 to A5 for the HS model, A7 to A11 for the HH model, A1' to A5' for the LS model, A7' to A11' for the LH model, on slope surface of four models subjected to X- direction shakings. The corresponding relative elevation h/H at each elevation is 0.0, 0.25, 0.5, 0.75 and 1.0. In general, along the slope elevation, the R_{PHA} tendency of four model slopes was rather the same, for the R_{PHA} was increasing with relative elevation h/H. Another observation is R_{PHA}, which demonstrated different change patterns between the upper and lower halves of the model slope. In the upper half (h/H > 0.5), R_{PHA} exceeded 1.2 and increased fast to its maximum at the slope crest, especially in two soft rock model slopes, indicating an obvious topographic amplification effect. The maximum crest amplification factor in the LS model, the HS model, the LH model, and the HH model was 3.3, 3.0, 2.2 and 1.6, respectively. In the lower half (h/H ≤ 0.5), most of R_{PHA} ranged between 1.0 and 1.2. Despite the overall increasing tendency of R_{PHA} in the lower half, its dependency on relative elevation was not as strong as in the upper part. In the HH model, R_{PHA} was always lower than 1.0 when h/H < 0.5, indicating an attenuation of the horizontal component response in the lower slope part. The response amplification at the slope crest and attenuation at the slope bottom were also found in other researches (Geli et al. 1988; Nguyen and Gatmiri 2007), and the explanation was the wave splitting and diffraction resulted in energy concentration at the (convex) crest and energy dissipation at the (concave) bottom. As the excitation intensity was increased from 0.1 g to 1.0 g, the differential response of R_{PHA} between the upper and lower halves seems not to change for each model slope.

The topographic amplification factor at the crest didn't exceed 2.0 for most of 2-D regular slope topography (Bouckovalas and Papadimitriou 2005; Assimaki et al. 2005; Nguyen and Gatmiri 2007). As an exception, Athanasopoulos et al. (1999) obtained a crest amplification factor of 5.6 in 2-D finite element model, relative to base motion with which the numerical response at the site behind the crest was close to the observed response during the 1995 Egion earthquake of Greece. The consistency was attributed to the simulated realistic topography and soil conditions. Based on a theoretical steep slope subjected to incident waves of different angles, Ashford and Sitar (1997) concluded that the time-domain amplification caused by topography (e.g. 1.4 for vertical incidence) was smaller than that caused by the natural frequency of free field behind the crest (e.g. 2.67 for vertical incidence). An overestimated amplification (e.g. 3.74 for vertical incidence) was obtained without separating the topographic and site effects, which was commonly noted in field

studies and many other studies. For the experimental topographic amplification presented here, the inconsistency in amplification level is caused also by the finite rigid boundary, as well as the soil nonlinearity ignored in numerical and theoretical models.

The change in the magnitude of the horizontal component response, R_{PHA}, with excitation intensity is detailedly shown as symbols in Figure 8 for all the monitoring points. The open symbols in the subfigure represent the R_{PHA} in the lower half of a model slope (h/H ≤ 0.5). When the excitation intensity was increased, R_{PHA} remained below 1.2, and the fine line, the average of R_{PHA} in the lower half, indicated no increase or only a minor increase of R_{PHA}. The phenomena show the magnitude of the horizontal component response in the lower half of each model slope was insensitive to the excitation intensity, regardless of the lithology and the slope structure. The solid symbols represent the R_{PHA} in the upper half of each model slope (h/H > 0.5). It can be seen R_{PHA} had larger value than that in the lower part, and the bold line, the average of R_{PHA} in the upper half, demonstrated different fluctuations in four model slopes as the excitation intensity got strengthened. When the excitation intensity was increased to 0.5 g, R_{PHA} in two hard rock models depicted a drastic increase, which corresponded to the sudden deterioration of internal structure of two models, as mentioned in the previous section. However, the sudden increase occurred when the excitation intensity equaled to 0.6 g for two soft rock models, and lagged behind the change of the internal structure. The hysteretic response of soft rock slope was confirmed by the Wangjiayan Landslide during the 2008 Wenchuan earthquake. The landslide with a volume of 1.4 million m3 took place within only about 10 minutes after the main earthquake, buried most of the old Beichuan area, and caused 1700 deaths (Xu et al. 2009).

After the abnormal point, R_{PHA} in the HS model began to decrease while R_{PHA} in the other three models increases, as the excitation intensity continued to increase. Normally, responses will be strengthened by the increase of excitation intensity and the narrowing gap between the resonance frequency of slope and the dominant frequency of input wave. The deterioration of internal structure of slope works in an opposite way. If the weakening effect surpasses the strengthening effect, decrease of R_{PHA} occurs just like in the HS model, otherwise, increase occurs as in the other three models.

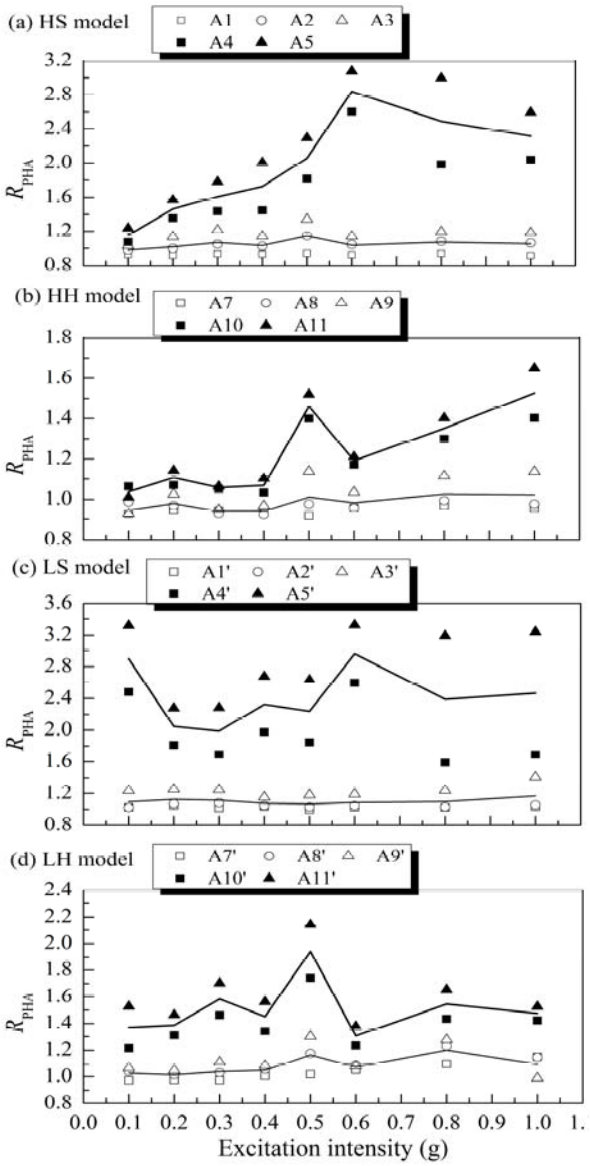

Figure 8 Responses to X- direction shaking: R_{PHA} versus excitation intensity. The bold line represents the average R_{PHA} in the upper half of each model slope, and the fine line represents the average R_{PHA} in the lower half of each model slope.

2.3 Effect of lithology

The ratio of PHA of the soft rock model slope to that of the hard rock model slope, R_{lith}, was calculated for two monitoring points on the slope surface and plotted along relative elevation h/H in Figure 9, under levels of shaking intensity in X-

direction. It can be seen that, the ratios between two homogeneous model slopes (R_{lith}^1) and the ratios between two layered model slopes (R_{lith}^2) were larger than 1.0 in the upper half of slope surface (h/H > 0.5), which indicated material of low strength produced stronger horizontal component response than material of high strength, not related to the slope structure. This result is well understood because material of low strength is more prone to arouse resonant response due to its smaller natural frequency which is close to the predominant frequency of earthquake waves. In relative elevation h/H ≤ 0.5, R_{lith}^1 > 1.0 still occurred. However, R_{lith}^2 <1.0 occurs as excitation intensity exceeded 0.5 g (included), during which the layered hard rock model (LH model) generated significant PHA response, coinciding with the observation in Figure 7. The possible explanation is the sharp change of its internal structure (represented by sharp drop of f in Figure 6) caused strong energy concentration in the lower part of LH model.

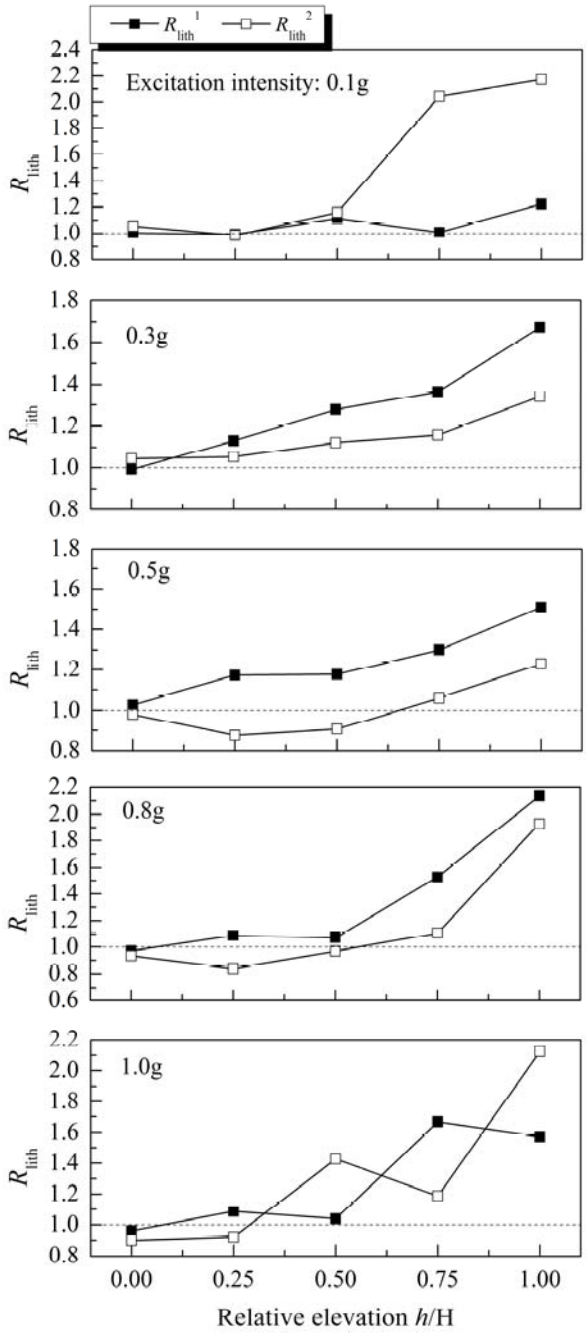

Figure 9 Ratio between PHAs of the soft rock model and the hard rock model, R_{lith}, versus relative elevation h/H under X- direction shaking

The R_{lith} versus relative elevation h/H curves show that effect of lithology (R_{lith}^1 and R_{lith}^2) was strengthened with increasing elevation on the slope surface. The maximum R_{lith}^1 reached 2.6 and the maximum R_{lith}^2 reached 2.4 at the slope top when the excitation intensity was 0.6 g (not shown in Figure 9). Model slopes composed of homogeneous materials obtained the stronger effect of lighology (i.e. R_{lith}^1 > R_{lith}^2) than model slopes with layered structure as the excitation intensity exceeded 0.3g.

2.4 Effect of structure

The ratio of PHA of the layered model slope to that of the homogeneous model slope, R_{stru}, was calculated for two monitoring points on the slope surface and plotted along relative elevation h/H in Figure 10, under levels of shaking intensity in X-direction. It can be seen that, the ratios between two hard rock model slopes (R_{stru}^1) were larger than 1.0 along the whole slope surface except when the excitation intensity reached 1.0 g, which indicated the LH model produced the stronger horizontal component response than the HH model. Further comparing two soft rock model slopes, the LS model also produced stronger response than the HS model when the excitation intensity was lower than 0.5 g (R_{stru}^2 > 1.0). As an explanation, on one hand, the horizontal discontinuities reduced the shear stiffness of the slope, and made the horizontal movement easier for layered slopes. On the other hand, severe wave diffraction occurred upon the discontinuities, thus produced more significant PHA response than the homogenous slope. Because of the vulnerability of low strength material to strong ground motion, it is reasonable

for it to suffer abnormal structural effect, so that R_{stru}^2 fluctuated around 1.0 when the excitation intensity was larger than 0.5 g, and response of the homogenous model even surpassed that of the layered one in some elevation.

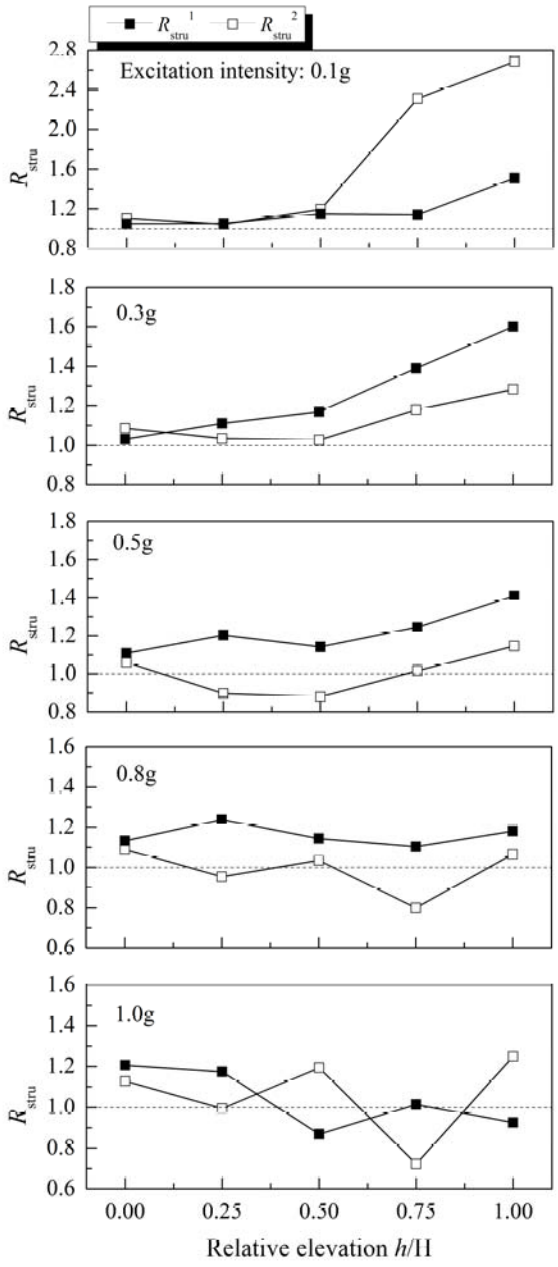

Figure 10 Ratio between PHAs of the layered model and the homogeneous rock model, R_{stru}, versus relative elevation h/H under X- direction shaking.

The R_{stru} versus relative elevation h/H curves show that effect of structure (R_{stru}^1 and R_{stru}^2) was strengthened with increasing elevation on the slope surface as the excitation intensity was lower than 0.5 g. After that, its dependence on the elevation was weakened. The maximum R_{stru}^1 reached 1.6 and the maximum R_{stru}^2 reached 2.7 at the slope top. Nonetheless, the model slopes composed of low -strength materials produced the stronger effect of structure (i.e. $R_{stru}^1 > R_{stru}^2$) than the model slopes composed of high -strength materials when the excitation intensity was between 0.2 g and 0.8 g.

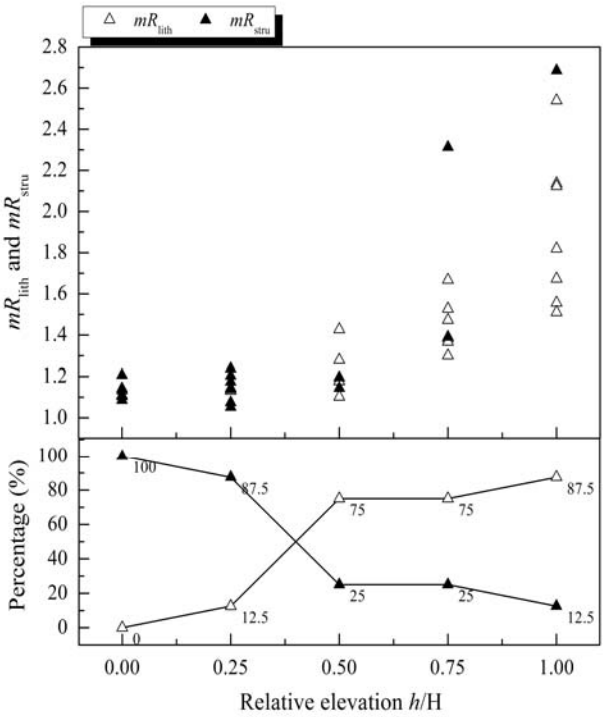

Figure 11 Distribution of the maximum R_{lith} (mR_{lith}) and R_{stru} (mR_{stru}) along the slope surface.

To compare the effect of lithology with the effect of structure on the horizontal component responses, a simple statistic calculation was made upon the above four ratios, R_{lith}^1, R_{lith}^2, R_{stru}^1 and R_{stru}^2. Firstly, the maximum R_{lith} (mR_{lith}=max{R_{lith}^1, R_{lith}^2}) and the maximum R_{stru} (mR_{stru}= max{R_{stru}^1, R_{stru}^2}) were obtained in each relative elevation h/H. Then, only the larger value between mR_{lith} and mR_{stru} in each h/H was plotted in the upper row of Figure 11. In this subfigure, the larger mR_{lith} is shown with the open symbols for all levels of excitation intensity from 0.1 to 1.0 g, while the larger mR_{stru} is shown with solid symbols. Finally, in each h/H, number of mR_{lith} or mR_{stru} was counted and the percentage of this number out of total number of mR_{lith} and mR_{stru} in this elevation was calculated and also plotted in the lower row of

Figure 11.

The lower figure shows mR_{stru} was mainly distributed in the lower half of the model slope with a percent over 85% (h/H < 0.5), and mR_{stru} in this slope part was smaller than 1.3. mR_{lith} was mainly distributed in the upper half with a percent over 75% (h/H ≥ 0.5), and majority of mR_{lith} had values higher than 1.3. That's to say, horizontal component responses in the lower and upper slope parts were seriously influenced by slope structure and lithology, respectively.

3 Conclusions

An experimental study was conducted on the seismic responses of four rock slopes, differing from lithology and slope structure, by means of a shaking table. The recorded Wenchuan earthquake waves were scaled to excite the model slopes. The study given here does not pretend to be complete for the considered slope surface (smooth, straight with only 60°), and beddings (even thickness, dip angle=0°) and homogeneous materials. The analysis focused on the acceleration responses to the horizontal component shakings in terms of the topographic effect, together with the influence of lithology and structure on this effect. The following conclusions can be drawn.

(1) The fundamental resonance frequency of each model slope decreased with the increasing excitation intensity, indicating a deterioration of the inner structure of the slope. The model simulating the hard rock slope had the higher resonance frequency than the model simulating the soft rock slope, and the homogeneous model slope also had the higher resonance frequency than the layered model slope.

(2) The amplification factor of peak horizontal acceleration (R_{PHA}) was increasing with relative elevation h/H of each model slope. The upper and lower halves of the model slope exhibited different change patterns of R_{PHA}, as R_{PHA} exceeded 1.2 and increased fast in the upper half (h/H > 0.5), but ranged below 1.2 in the lower half, indicating an obvious topographic amplification effect.

(3) The amplification factor R_{PHA} in the lower half of each model slope was independent of the excitation intensity and kept fairly stable. The sudden increase of R_{PHA} in the upper half corresponded to the drastic deterioration of the inner structure of the model slope.

(4) The model simulating the soft rock slope produced the larger R_{PHA} than the model simulating the hard rock slope, especially in comparison between two layered model slopes. The effect of lithology was strengthened with increasing elevation.

(5) The layered model slope produced the larger R_{PHA} than the homogeneous model slope, especially in comparison between two models simulating the hard rock slopes. The effect of structure was strengthened with increasing elevation in weak motions.

(6) Considering the nonlinear topographic amplification of PHA, the upper half of a slope was influenced more seriously by the effect of lithology, while the lower half was influenced more seriously by the effect of slope structure.

Acknowledgements

This research is financially supported by the National Basic Research Program "973" Project of the Ministry of Science and Technology of the People's Republic of China (Grant No. 2013CB733200), the National Science Found for Distinguished Young Scholars of China (Grant No. 41225011), the Chang Jiang Scholars Program of China and the open fund on "Research on large-scale landslides triggered by the Wenchuan earthquake" provided by the State Key Laboratory of Geohazard Prevention and Geoenvironment Protection. We thank Mr. ZOU Wei, CHEN Long, and WANG Long who assisted in the tests. The authors also thank all reviewers whose comments greatly improved the quality of the manuscript.

References

Ashford SA, Sitar N (1997) Analysis of topographic amplification of inclined shear waves in a steep coastal bluff. Bulletin of the Seismological Society of America 87: 692-700.

Assimaki D, Gazetas G, Kausel E (2005) Effects of local soil

conditions on the topographic aggravation of seismic motion: parametric investigation and recorded field evidence from the 1999 Athens Earthquake. Bulletin of the Seismological Society of America 95: 1059-1089. DOI: 10.1785/0120040055

Athanasopoulos GA, Pelekis PC, Leonidou EA (1999) Effects of surface topography on seismic ground response in the Egion (Greece) 15 June 1995 earthquake. Soil Dynamics and Earthquake Engineering 18:135-149. DOI: 10.1016/S0267-7261(98)00041-4

Beresnev IA, Wen KL, Yeh YT (1995) Seismological evidence for nonlinear elastic ground behaviour during large earthquakes. Soil Dynamics and Earthquake Engineering 14:103-114. DOI: 10.1016/ 0267-7261(94) 00036-G.

Bouckovalas GD, Papadimitriou AG (2005) Numerical evaluation of slope topography effects on seismic ground motion. Soil Dynamics and Earthquake Engineering 25:547-558. DOI: 10.1016/j.soildyn.2004.11.008

Bozzano F, Lenti L, Martino S, et al. (2011) Earthquake triggering of landslides in highly jointed rock masses: reconstruction of the 1783 Scilla rock avalanche (Italy). Geomorphology 129: 294-308. DOI: 10.1016/j.geomorph.2011.02.025

Chen Y, Li L, Li J, Li G (2009) Wenchuan earthquake: way of thing is changed. Episodes 31: 374-377.

Chigira M, Wu XY, Inokuchi T,Wang GH (2010) Landslides induced by the 2008 Wenchuan earthquake, Sichuan, China. Geomorphology 118: 225-238. DOI: 10.1016/j.geomorph.2010.01.003

Cui P, Zhu YY, Han YS, et al. (2009) The 12 May Wenchuan earthquake-induced landslide lakes: distribution and preliminary risk evaluation. Landslides 6:209-223. DOI: 10.1007/s10346-009-0160-9

Curtis WD, Logan JD, Parker WA (1982) Dimensional analysis and the pi theorem. Linear Algebra and its Applications 47: 117-126. DOI:10.1016/0024-3795(82)90229-4

Del GV, Wasowski J (2007) Directivity of slope dynamic response to seismic shaking. Geophysical Research Letters 34: L12301.

Dong JY, Guo X, Wu FQ, Qi SW (2011) The large-scale shaking table test study of dynamic response and failure mode of bedding rock slope under earthquake. Rock and Soil Mechanics 32: 2977-2983. (In Chinese)

Ducellier A, Aochi H (2012) Interactions between topographic irregularities and seismic ground motion investigated using a hybrid FD-FE method. Bulletin of Earthquake Engineering 10: 773-792. DOI: 10.1007/s10518-011-9335-6

Geli L, Bard PY, Jullien B (1988) The effect of topography on earthquake ground motion: a review and new results. Bulletin of the Seismological Society of America 78: 42-63.

Harp EL, Jibson RW (1996) Landslides triggered by the 1994 Northridge, California earthquake. Bulletin of the Seismological Society of America 86: S319-S332.

Harp EL, Jibson RW (2002) Anomalous concerntrations of seismically triggered rock falls in Pacoima Canyon: are they caused by highly susceptible slopes or local amplification of seismic shaking? Bulletin of the Seismological Society of America 92: 3180-3189. DOI: 10.1785/0120010171

Hatzor YH, Arzi AA, Zaslavsky Y, Shapira A (2004) Dynamic stability analysis of jointed rock slopes using the DDA method: King Herod's Palace, Masada, Israel. International Journal of Rock Mechanics and Mining Science 41: 813-832. DOI: 10.1016/j.ijrmms.2004.02.002

Hong YS, Chen RH, Wu CS, Chen JR (2005) Shaking table tests and stability analysis of steep nailed slopes. Canadian Geotechnical Journal 42: 1264-1279. DOI: 10.1139/T05-055

Huang RQ, Fan XM (2013) The landslide story. Nature Geoscience 6: 325-326. DOI:10.1038/ngeo1806

Huang RQ, Li WL (2008) Research on development and distribution rules of geohazards induced by Wenchuan earthquake on 12th May 2008. Chinese Journal of Rock Mechanics and Engineering 27: 2585-2592. (In Chinese)

Keefer DK (1984) Landslides caused by earthquakes. Geological Society of America Bulletin 95: 406-421. DOI: 10.1130/0016-7606(1985)96<1093:LCBEDA>2.0.CO;2

Liang Q, Han W, Ma R, Chen W (2005) Physical simulation study on dynamic failures of layered rock masses under strong ground motion. Rock Soil and Mechanics 26: 1307-1311. (In Chinese)

Lin ML, Wang KL (2006) Seismic slope bahavior in a large-scale shaking table model test. Engineering Geology 86: 118-133. DOI: 10.1016/j.enggeo.2006.02.011

Ling HI, Mohri Y, Leshchinsky D, et al. (2005) Large-scale shaking table tests on modular-block reinforced soil retaining walls. Journal of Geotechnical and Geoenvironmental Engineering 131: 465-476. DOI: 10.1061/(ASCE)1090-0241(2005)131:4(465)

Louis B (1957) The pi theorem of dimensional analysis. Archive for Rational Mechanics and Analysis 1: 35-45.

Nguyen KV, Gatmiri B (2007) Evaluation of seismic ground motion induced by topographic irregualrity. Soil Dynamics and Earthquake Engineering 27: 183-188.

Shimizu Y, Aydan ö, Ichikaw Y (1988) A model study on dynamic failure modes of discontinuous rock slopes. In: Li CX, Yang L (Eds.), Proceedings of the International Symposium on Engineering in Complex Rock Formations, Beijing, 3-7 November, 1986. Beijing: Science Press.

Qi SW, Xu Q, Lan HX, et al. (2010) Spatial distribution analysis of landslides triggered by 2008.5.12 Wenchuan earthquake, China. Engineering Geology 116: 95-108. DOI: 10.1016/j.enggeo.2010.07.011

Wang KL, Lin ML (2011) Initiation and displacement of landslide induced by earthquake - a study of shaking table model slope test. Engineering Geology 122: 106-114. DOI: 10.1016/j.enggeo.2011.04.008

Wartman J, Seed RB, Bray JD (2005) Shaking table modeling of seismically induced deformations in slopes. Journal of Geotechnical and Geoenvironmental Engineering 610-622. DOI: 10.1061/(ASCE)1090-0241(2005)131:5(610)

Wen ZP, Xie JJ, Gao MT, Hu YX (2010) Near-source strong ground motion characteristics of the 2008 Wenchuan Earthquake. Bulletin of the Seismological Society of America 100: 2425-2439. DOI: 10.1785/0120090266

Whitman RV, Lambe PC (1986) Effect of boundary conditions upon centrifuge experiments using ground motions simulations. Geotechnical Testing Journal 9: 61-71. DOI: 10.1520/GTJ11031J

Xu Q (2009) Main types and characteristics of the geo-hazards triggered by the Wenchuan earthquake. Journal of Geological Hazards and Environment Preservation 20: 86-93. (In Chinese)

Xu Q, Pei XJ, Huang RQ (2009) Large-scale landslides induced by the Wenchuan earthquake. Beijing: Science Press. (In Chinese)

Yang J, Sato T, Savidis S, Li XS (2002) Horizontal and vertical components of earthquake ground motions at liquefiable sites. Soil Dynamics and Earthquake Engineering 22: 229-240. DOI: 10.1016/S0267-7261(02)00010-6

Ye B, Ye GL, Ye WM, Zhang F (2013) A pneumatic shaking table and its application to a liquefaction test on saturated sand. Natural Hazards 66: 375-388. DOI: 10.1007/s11069-012-0489-6